Flow, Turbulence and Combustion manuscript No.
(will be inserted by the editor)

DNS of a single low-speed streak subject to spanwise wall oscillations

Prabal Singh Negi · Maneesh Mishra · Martin Skote

Received: date / Accepted: date

Abstract Direct numerical simulation (DNS) is performed to study the effect of steady streamwise oscillations of the spanwise wall velocity on a single low-speed streak in a laminar boundary layer. The low-speed streak is numerically generated by simulating a screen which creates a momentum loss. The wall oscillations are shown to reduce the skin friction which drops below the laminar Blasius flow value (without the presence of streaks) for certain cases of wall oscillations. In addition, the peak streamwise velocity fluctuation of the streaks are reduced drastically by up to 90%, the trend in reduction being monotonic with respect to higher amplitude oscillations. The effect of oscillation is also studied during transition (breakdown of the streak) and it is found that the optimum wavenumber of the oscillation changes by nearly an order of magnitude during transition. The reduction of peak streamwise velocity fluctuations shows a phase dependent behaviour which is explained based on the regeneration of turbulence in the absence of a streamwise gradient of the spanwise velocity. The general trend of reduction in streamwise fluctuations across different wavenumbers does not correlate well with the decrease in skin friction. A much better qualitative correlation is found when comparing the relative trends for skin friction and wall-normal velocity fluctuations for different oscillation wavenumbers.

Keywords Transition control · DNS · laminar streaks · wall oscillation

M. Skote
School of Mechanical and Aerospace Engineering, Nanyang Technological University,
50 Nanyang Avenue, Singapore 639798
Tel.: +65-6790-4271
E-mail: mskote@ntu.edu.sg

1 Introduction

Drag reduction is an important goal in many engineering applications. Strategies for achieving drag reduction are broadly classified as either active or passive. Active mechanisms are further classified as closed loop or open loop type. Spanwise wall oscillation is one such active mechanism for achieving high drag reductions. The mechanism has an attractive property of being open loop, i.e. not requiring a feedback law, and thus lends itself suitable for practical implementation without the need for complicated sensors to detect the flow state. In recent years the spanwise wall oscillation mechanism has gathered much attention due to very high drag reductions that are achievable. The phenomenon of drag reduction using spanwise wall oscillations was first reported by Jung et al.[19] and Akhavan et al.[1]. It had already been shown previously that the introduction of a sudden spanwise pressure gradient in a two-dimensional turbulent flow temporarily suppresses the production of turbulence. The suppression, however, was temporary since the flow eventually adjusted to the new state and the turbulence suppression was lost. Jung et al.[19] used this idea to create a sustained suppression of turbulence. They performed direct numerical simulation (DNS) of channel flow subjected to oscillatory spanwise crossflow or spanwise oscillation of one of the channel walls and reported a 40% attenuation in wall shear stress and also a significant reduction in other turbulent quantities. The wall oscillations were implemented by prescribing a spanwise velocity at one of the walls of the type:

$$W_{wall} = W_m \sin(\omega t). \tag{1}$$

where ω is the frequency of spanwise oscillations and W_m is the maximum velocity of the wall. Additionally, the spanwise averaged component of the flow was found to remain in agreement with the laminar flow solution [19]. This particular feature was consistently found in subsequent studies as well [10,36], attributed to the small height of the Stokes layer for the optimal oscillation parameters, confining it primarily to the viscous sublayer. Ricco and Quadrio [28] provide further explanations for this agreement based on the vanishing $\partial\overline{v'w'}/\partial y$ term in the spanwise momentum equation. Interest of the community was piqued by Baron and Quadrio [5] when they reported a net positive energy balance from their DNS study for this type of wall forcing. The authors considered the energy loss to drive an idealized system against the viscous forces of the flow and found that the net energy saved from the wall oscillations was slightly positive for low amplitude oscillations. However, the simulations were only done for one particular oscillation frequency. They also reported an upward shift of the logarithmic layer. In addition, they noted that the streamwise velocity fluctuations are only marginally reduced when normalized by the frictional velocity of the perturbed case. Laadhari et al. [20] conducted an experimental study for boundary layer flow in which they confirmed the reduction of the gradient of the streamwise velocity near the oscillating wall. Yudhistira and Skote [39] performed the first DNS for boundary layer flows over an oscillating wall and achieved about a 40% drag reduction.

They also showed that the spatial development of drag reduction was similar to that observed in the experiments [11,29,20]. An experimental study was done by Choi et al. [11] for boundary layer flows where they realized a 45% reduction in skin friction drag. The authors proposed a conceptual model for the drag reduction based on the realignment of the streamwise streaks in the spanwise direction. Choi [10] later built on this conceptual model of vorticity realignment showing reduction in streamwise vorticity near the wall leading to reduced burst activity and consequently lower turbulent drag.

Since then several studies have followed focusing on different aspects of the phenomenon. For example, Quadrio and Ricco [23] studied the initial transient response on suddenly imposed oscillations. The same authors also performed a parametric study on the drag reduction in channel flow showing an optimum oscillation period T^+ lying between 100 and 125 [23], where $^+$ denotes scaling using the frictional velocity u_* and the kinematic viscosity ν. On the other hand, at a constant T^+ the drag reduction saw a logarithmic increase with spanwise wall velocity W^+_{wall}. The energy savings however remained positive only for small $W^+_{wall} < 7$ amplitude oscillations. Xu et al. [38] analyzed the transient response of the Reynolds stress transport term and showed a hindrance to the inter-component turbulence kinetic energy transfer, leading to turbulence suppression. Skote [32] pointed out several differences and similarities between the temporal transients in channel flow and the spatial transients in boundary layer flow.

As the temporal oscillations according to (1) lead to relatively small energy gains when balanced by an idealized actuator [5], Viotti et al. [36] used the convection velocity of the near wall turbulent structures to replace the temporal oscillations with an equivalent steady spatial oscillation of the spanwise velocity. Under space-time conversion the wall forcing took the form:

$$W_{wall} = W_m \sin(kx). \tag{2}$$

where k is the wavenumber of the wall forcing and x the streamwise coordinate. They showed that the time harmonic and spatial cases to be analogous with the optimum wavelength remaining the same under space time conversion. The spatial oscillations however produced higher net energy savings. The spatial forcing was also shown to yield similar positive net energy saving for boundary layer flows as shown by Skote [31] who also demonstrated a phase dependence of drag reduction on the spanwise wall velocity phase. Furthermore, Skote [33] showed the improved energy budget for spatial oscillations can be explained by the turbulence production term involving the streamwise gradient of the wall forcing velocity. The same author [34] recently demonstrated that the scaling of the velocity profile remains identical for the two different types of forcing.

More shape forms of the forcing have since been studied, some of which may not strictly be considered as wall forcing [13] [14]. Travelling waves were used by Quadrio et al.[25] as a form of wall forcing which exhibited an unexpectedly rich behaviour showing both drag reduction as well as drag increase depending on the parameters of the travelling wave. They also showed that the net energy savings for travelling waves were higher than purely temporal as well as purely

spatial oscillation of the wall which could go as high as 26% at low amplitude oscillations. The form of wall forcing used by Quadrio et al. was:

$$W_{wall} = W_m \sin(kx + \omega t). \tag{3}$$

Touber et. al. [35] provide an excellent review of the past works and go on to show turbulence suppression in different quadrants for phase averaged statistics for temporal oscillations. They also show an effect of the outer layer structures on the drag and thus point to possible degradation of the drag reduction mechanism at higher Reynolds numbers.

More recently the idea of spanwise oscillation has been applied to the suppression of growth of low-speed streaks in the laminar boundary layer. These streaks occur due to the growth of disturbances in the laminar boundary layer [2] which can become sufficiently strong to trigger transition to turbulence[8, 3,17,30], by-passing the classical route of exponentially growing unstable TS waves. Some of the earlier work can be found in the PhD thesis of Berlin [6] where temporal spanwise oscillations are used to delay transition due to oblique waves. Ricco [27] studied the evolution of laminar streaks subjected to steady spanwise wall oscillations using the linearized unsteady boundary region equations (LUBR). Under the linearized conditions he showed substantial reduction of the velocity fluctuations. Hack and Zaki [16] studied the continuous modes of the Orr-Sommerfeld spectrum in the laminar boundary layer under time-harmonic shear at the lower wall, showing substantial reduction of the free-stream disturbance entering the boundary layer. Dong and Wu [12], however, question the physical meaning of the continuous modes and and their use in modelling the free stream vortical disturbances penetrating the boundary layer. The authors showed that at finite Reynolds number these disturbances are characterized by a different type of continuous spectrum, whose eigenfunctions exponentially increase away from the wall.

Jovanovic [18] used the linearized Navier-Stokes equations to show large reduction in the ensemble energy densities of transitional Couette and Poiseuille flows under small amplitude transverse oscillations. Rabin et. al. [26] used a newly developed non-linear variational method to show that the minimum initial disturbance to trigger transition to turbulence is substantially increased in plane Couette flow in the presence of temporal spanwise wall oscillations. Despite these studies, a fully non-linear simulation of transitional flows under wall oscillation control remains lacking. Furthermore, the effectiveness of the spanwise oscillations during the transition stage remains an open question. It is yet unknown if the transition process can be suppressed with the oscillation mechanism. Consistency of the parameters across different flow regimes (laminar, transition and fully turbulent), is another question which yet remains to be addressed.

In the current study, the effect of steady spanwise oscillations on laminar streaks is studied using DNS. Asai et al. [4] in their experimental study generated a single low-speed streak to study its stability characteristics. The streak is generated by the use of a small screen set normal to the wall around the

middle (spanwise) of the boundary layer plate and downstream of the leading edge. The entire experimental setup was numerically replicated by Brandt [7]. We have used a similar methodology to numerically generate the a low-speed streak and study the effect of spatial wall oscillation on the generated streak. The effect of oscillations is further studied during transition to turbulence, which is artificially triggered using time periodic blowing and suction at the wall, with the aim of investigating the possibility of stabilizing the perturbed streak, or delaying the transition process, by using an open loop control method (steady spanwise wall oscillations) which has proven efficient for turbulence suppression. Phase relationship of fluctuating velocity components with the spanwise flow are further explored. However, the scope of the current paper is limited to exploring the differences in the spanwise forcing effectiveness in laminar and transitional regimes, while the conceptual explanations behind the drag mechanism itself has been left for a future study.

The remainder of the paper is organized as follows - section 2 describes the numerical method used in the study. In section 3 the created low-speed streak is validated by previous experimental data. Section 4 shows the results of wall oscillation on the low-speed streak while section 5 presents the details of oscillation in the transition region. The results are summarized and concluded in section 6.

2 Numerical Setup

The DNS code used in this study was developed at KTH, Stockholm [9]. It is based on spectral method to solve the three-dimensional, time dependent, incompressible Navier-Stokes equations. The algorithm uses Fourier representation in the streamwise and the spanwise directions, and Chebyshev polynomials in the wall-normal direction. The algorithm is based on a pseudo-spectral treatment of the non-linear terms with multiplications of those terms calculated in physical space to avoid the sum of convolution terms. Fast Fourier Transform (FFT) is used for the transformation between physical and spectral space. For the time advancement of the nonlinear terms, a four-step, low storage third order Runge-Kutta method is used while a second order Crank-Nicolson method is used for the advancement of the linear terms. Aliasing error from the evaluation of non-linear terms are removed by the 3/2 rule for FFT calculations in wall-parallel planes while in the wall-normal direction, increasing spatial resolution has been found to be more efficient than dealiasing. In order to account for the downstream boundary layer growth, a spatial technique is found to be necessary. The requirement is combined with the periodic boundary condition in the streamwise direction by the use of a fringe region. This region is implemented at the downstream end of the computational domain, where a volume forcing is added to the flow using a function $\lambda(x)$, which is smoothly raised from zero such that the flow is forced to a desired solution v. The volume forcing term is:

$$F = \lambda(x)(v - u) \tag{4}$$

where v is the laminar boundary layer to which the solution is forced to. The forcing vector is smoothly changed from a laminar boundary layer profile at the beginning of the fringe region to the desired outflow conditions at the end of the fringe region. This laminar profile is identical to the inflow condition at the beginning of the computational region, hence periodic boundary condition in the streamwise direction applies. The fringe function used is of the kind:

$$\lambda(x) = \lambda_{max}\left[S\left(\frac{x - x_{start}}{\triangle_{rise}}\right) - S\left(\frac{x - x_{end}}{\triangle_{fall}} + 1\right)\right] \tag{5}$$

where S(a) is a smooth step function defined as:

$$S(a) = \begin{cases} 0, & a \leq 0 \\ 1/\left[1 + \exp\left(\frac{1}{a-1} + \frac{1}{a}\right)\right], & 0 < a < 1 \\ 1, & a \geq 1 \end{cases} \tag{6}$$

The length scale used for the normalization is based on the inlet displacement thickness, δ^*, the velocity scale used is the inlet free stream velocity, U_∞, and time is normalized using δ^*/U_∞.

Asai et. al., in their experimental setup study the flow over a boundary layer plate placed parallel to the oncoming flow of the wind tunnel test section. In order to create a single low-speed streak, a 40-mesh wire-gauze screen is placed 500mm downstream of the elliptical leading edge of the plate. The wire-gauze screen has a porosity of 0.7 is set normal to the plate. The height is kept close to the displacement thickness of the laminar boundary layer without the screen. Further details of the setup is given in [4]. In order to simulate the screen in the current study a momentum loss is induced in the near wall region of the Blasius boundary layer using a localized volume forcing, added to the streamwise component of the momentum equation. The forcing of the form:

$$F(x, y, z) = A_x S\left(\frac{y_{loc} + y_{scale} - y}{y_{scale}}\right)\left(\frac{y}{y_{loc}} - \frac{u}{u_f}\right)u_f S\left(\frac{t}{t_{scale}}\right) g\left(x, z\right), \tag{7}$$

with

$$g(x, z) = \exp\left[-\left(\frac{x - x_{loc}}{x_{scale}}\right)^2\right] \times \left[S\left(\frac{z + z_{loc} + z_{scale}/2}{z_{scale}}\right) - S\left(\frac{z - z_{loc} + z_{scale}/2}{z_{scale}}\right)\right] \tag{8}$$

where S(a) is the same step function as defined for the fringe region. u_f is the value of u attained at a distance y_{loc} from the wall where the forcing starts decaying to zero in y_{scale}. The forcing location is around x_{loc} corresponding

to the location of the screen in the experiment and has an extent of z_{loc}. z_{scale} is used so as to smoothly raise or reduce the forcing so that a higher grid resolution is not required to resolve the solution. Table 1 shows the values of the parameters used to create the low-speed streak. In the numerical study by Brandt [8], there are two values for z_{loc} which correspond to the 7.5mm and the 5mm wide screens. In our study we have only considered the case for the 7.5mm screen and hence only one value of z_{loc} has been used.

Table 1: Parameter Values

Parameter	value	Parameter	value	Parameter	value
y_{loc}	1	z_{loc}	1.82	x_{scale}	1.4
y_{scale}	0.4	z_{scale}	0.35	u_f	0.07
x_{loc}	57.19	A_x	0.8	t_{scale}	300

The displacement thickness based Reynolds number of 549.35 at the inlet has been used so as to match the Reynolds number for the experimental study [4] at the location of the screen (taking into account its downstream growth between the inlet and x_{loc}). The computational domain for the simulation was set at 450, 15 and 9 units in the streamwise, spanwise and wall-normal directions based on the inlet displacement thickness δ^*. The fringe region was set to $50\delta^*$ units right before the end of the computational domain. The resolution of the study was set to 512x73x96 (RES1), representing 512 streamwise and 96 spanwise Fourier modes, and 73 Chebyshev modes in the wall-normal direction. The simulation was checked against two more cases run with 612x73x128 (RES2) and 800x91x128 (RES3) Fourier/Chebyshev modes. There was no appreciable difference found in the statistics of the converged flow. All subsequent laminar streak cases were run with RES1 as that proved to be sufficient to resolve the flow. Flow convergence was carefully checked manually by comparing the averaged statistics for different time intervals. Oscillations with higher amplitudes were found to take longer for statistical convergence. For high amplitude cases the flow was found to be statistically stable by 8000 time units. The simulation was further translated to 10000 time units and all statistics from the final 2000 time units are reported herein. All statistical quantities presented are spanwise averages unless specifically mentioned otherwise.

The streak generated by the simulated screen represents a stable streak which undergoes substantial viscous decay and thus no natural transition is observed. In order to trigger a transition of the streak, secondary instabilities are generated by localized time-periodic blowing and suction at the wall. The blowing and suction are implemented by applying a time harmonic wall-normal velocity at the wall, the extent of which has been localized to a small region by using an exponential decay in the x and z directions for the amplitude of the blowing and suction. The function for the wall-normal velocity is:

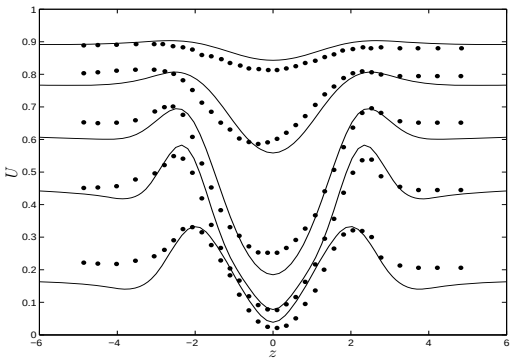

Fig. 1: Spanwise modulation of streamwise velocity at $x = 81$. Lines represent the values obtained in the current study and the dots show the corresponding experimental values in [4]. The curves from bottom to top represent mean streamwise velocity values at $y = 0.5, 1, 1.5, 2$ and 2.5 respectively.

$$v_{var}(x, 0, z) = v_{wall} \exp\left[-\left((x - x_{sb})/x_{sc}\right)^2\right] \exp\left[-(z/z_{sc})^2\right] \sin(\omega t), \quad (9)$$

where v_{var} is the wall-normal velocity having a maximum amplitude of $v_{wall} = 0.035$ at the wall at $x = x_{sb} = 110$ and $z = 0$ (midpoint of the plane). $x_{sc} = 2.5$ and $z_{sc} = 0.5$ represent the extent of the wall-normal velocity region of blowing and suction and $\omega = 0.36$ is the frequency of the blowing and suction. All transition cases were run at the highest resolution with 800x91x128 (RES3) Fourier/Chebyshev modes.

In addition, the spanwise size of the computational box was doubled for one simulation of a transition case, and no significant difference in the streamwise development of the flow could be detected. The maximum deviation detected in velocity fluctuations ($rms-$values) was 7%, while the wall-normal profiles in all other aspects remained identical, for all streamwise positions. Hence, it was concluded that the smaller computational box was wide enough to capture the downstream development accurately.

3 Streak validation

The numerically generated streak has been compared with the experimental values obtained by Asai et al. [4]. Figure 1 shows the spanwise distribution of the streamwise velocity at $x = 81$ as obtained in the current study. The dots represent experimental values obtained in [4]. The streamwise velocity patterns shows the characteristic profile observed in laminar streaks where the low-speed fluid is uplifted to the upper part of the boundary layer and high-speed fluid is in turn displaced to the lower portion of the boundary layer. Similar results were obtained by Brandt [7]. All features of the experimental setup [4] and the numerical study [7] have been successfully reproduced in the current simulation work.

The plot of u_{rms}/u_{rms}^{max} at different downstream locations against the wall-normal coordinate normalized by the displacement thickness (Figure 2) shows that the maxima of the streamwise velocity fluctuations lies very close to

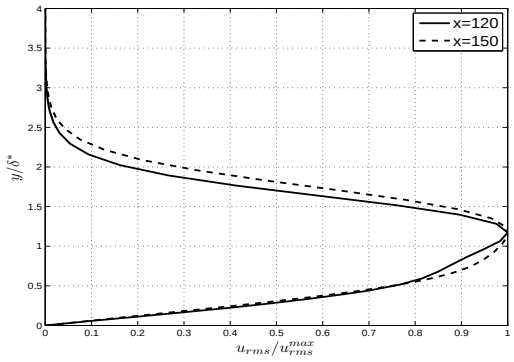

Fig. 2: Wall-normal profile of streamwise fluctuations (normalized by their peak values) obtained which is characteristic of streaks in a laminar boundary layer

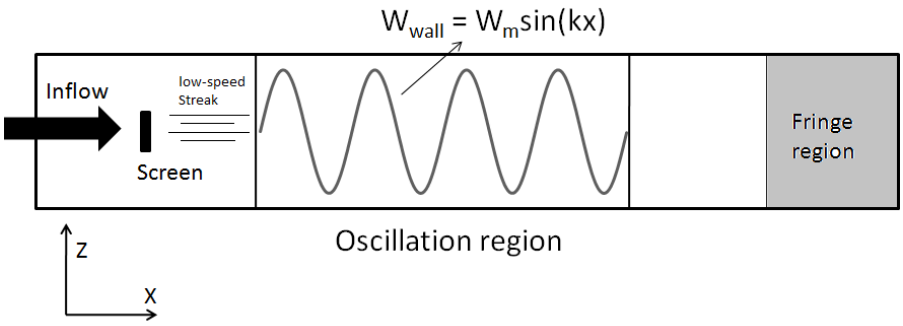

Fig. 3: Schematic of wall oscillation implementation

$1.3\delta^*$ which is characteristic of streaks in a laminar boundary layer as shown in earlier DNS [2,21] as well as in experiments [37,22]. Overall, the numerical technique is successful in generating a low-speed streak which is similar to the one generated by the penetration of free-stream disturbances into the laminar boundary layer.

4 Streak response to wall oscillations

The oscillation at the wall assumes a simple trigonometric form for the spanwise velocity according to equation (2).

The wall oscillations was implemented in the domain from $x = 90$ to $x = 300$. The region was selected such that the start of the oscillation is sufficiently downstream of the simulated screen and the end point of the oscillations is sufficiently upstream of fringe region. A schematic of the wall oscillation is shown in Figure 3.

A parametric study of the effect of changing wavenumber (k) and maximum spanwise velocity (W_m) has been performed. The parameters are varied from $0.03 < k < 0.75$ and $0.16 < W_m < 0.6$. The wall-normal Stokes layer profile at

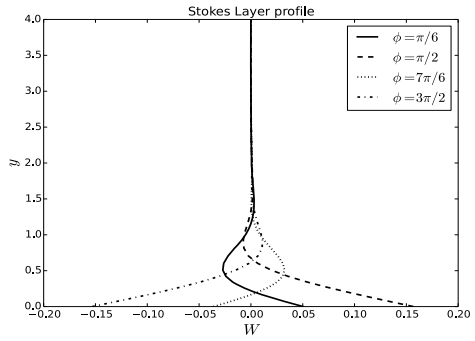

Fig. 4: Stokes profile for $W_m = 0.16$ and $k = 0.12$

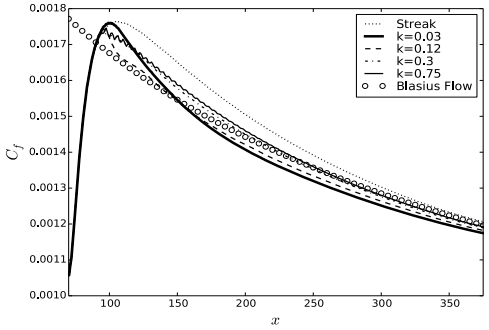

Fig. 5: The reduction of C_f due to spanwise wall oscillations

different locations is first depicted in Figure 4 for $W_m = 0.16$ and $k = 0.12$. The locations ($x = 199.51, 208.30, 225.88, 234.67$) correspond to the wall phase of $\phi = \pi/6, \pi/2, 7\pi/6$ and $3\pi/2$ in the third wavelength of oscillation. The Stokes layer stays confined within the laminar boundary layer which, at the start of the oscillation rises to $\delta_{99} = 3.3$. The Stokes layer height decreases with higher wavenumbers and thus confining it closer to the wall region. Even for the lowest wavenumber used in the parametric study, the Stokes layer remains confined within the boundary layer. The Stokes layer was also investigated for the case of flow without a streak and the profile remains nearly identical to the one with the streak.

In previous studies [24,36,5] on turbulent flow under wall oscillation it was observed that drag reduction followed a monotonic behaviour with the maximum oscillation amplitude. On the other hand, the frequency of temporal oscillations had an optimum value beyond which the effectiveness of the mechanism diminished. The analogous case of spatial oscillations also displayed an optimum wavenumber for peak drag reduction. Similar behavior was reported by Ricco [27] in the linearized study of streaks under oscillation. In order to find the optimum wavenumber in the current study, the oscillation amplitude was kept constant at $W_m = 0.16$ and the wavenumber k of wall oscillation was varied from 0.03 to 0.75.

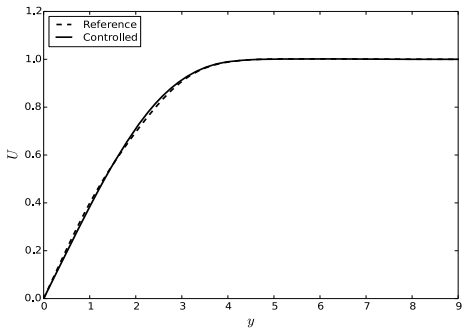

Fig. 6: Streamwise velocity profile for $W_m = 0.16$ and $k = 0.03$

For the case of laminar streaks, the effect of oscillation on the wall drag remains small. Figure 5 shows the trend of the skin friction coefficient (C_f) values under different oscillation cases. While there is a slight reduction of the wall shear stress from the reference value (without oscillations), the difference is small. A closer view (not shown) reveals that lower wavenumbers create a relatively larger reduction in C_f. However, the relative difference between different oscillation cases is small. Interestingly, for $k = 0.03$ and 0.12 the skin friction coefficient drops below the two-dimensional laminar Blasius flow which is given by $C_f = 0.664/\sqrt{Re_x}$.

As can be expected from the results of the C_f curves, the effect of oscillation on the base flow is extremely small. Figure 6 shows the mean streamwise velocity profile for one of the cases at $x = 195$, which is within the control region. The profiles of the controlled and the uncontrolled flows are almost indistinguishable, even for the wavenumber that showed the most promising C_f reduction. Only one position is shown in the figure for clarity, however multiple positions and different wavenumber cases were investigated and for all cases the change in the base flow was found to be minor as depicted by Figure 6.

On the other hand, the peak values of streamwise velocity fluctuations are substantially suppressed (Figure 7), reducing to about 25% of their original values. The trend is monotonic with the lower wavenumbers showing greater reduction in fluctuations. To make the comparison with the reference case clearer, figure 8 shows the trend of $\widetilde{u}^{max}$, where we have defined $\widetilde{u}^{max}$ as the ratio of the peak streamwise velocity fluctuations for the oscillated and non-oscillated cases. The reduction to 25% for $k = 0.03$ is clearly visible from the graph. An optimum wavenumber was however not obtained within the current range of wavenumbers. It was not possible to check for lower wavenumbers due to the limitation of the computational box size. The lowest wavenumber with $k = 0.03$ corresponds to a streamwise wavelength of 210 which covers nearly 50% of the computational domain.

Along with the reduction in fluctuations the locations of the peak fluctuations are shifted away from the wall and the trend shows a monotonic behaviour with the shift being the highest for the lowest wavenumber studied

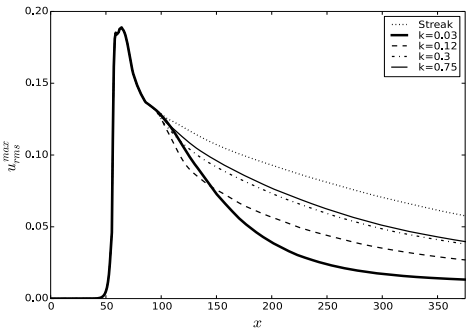

Fig. 7: Peak u_{rms} values along the streamwise coordinate for the reference case (without oscillation) and the oscillated cases with $k = 0.03$, 0.12, 0.3 and 0.75

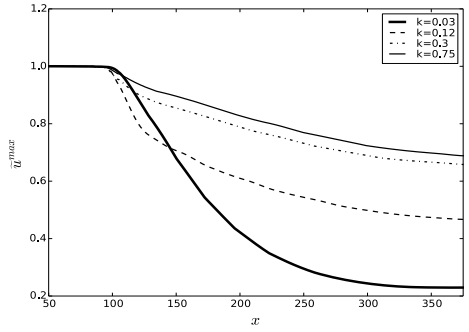

Fig. 8: $\widetilde{u}^{max}$ for $k = 0.03$, 0.12, 0.30 and 0.75 at $W_m = 0.16$

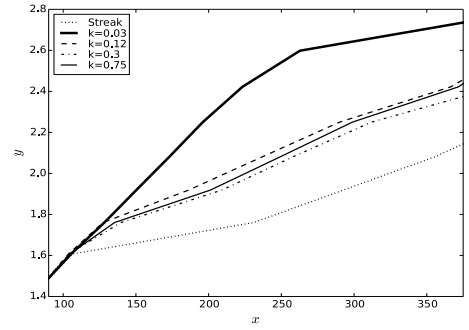

Fig. 9: Outward shift in the wall-normal location of peak streamwise fluctuations

(Figure 9). The exception being for the highest wavenumber case ($k = 0.75$) for which the shift of peak locations was higher than for the case of $k = 0.30$. Jung et al. [19] had reported similar shift of peak values away from the wall towards the center of the channel for turbulent channel flows. An upward shift of the log-law layer has also been reported in turbulent flow cases attributed to the thickening of the viscous sub-layer[5,36].

Higher amplitude oscillations were studied for $k = 0.03$ which showed a trend of monotonic rise in velocity fluctuation reduction with peak wall

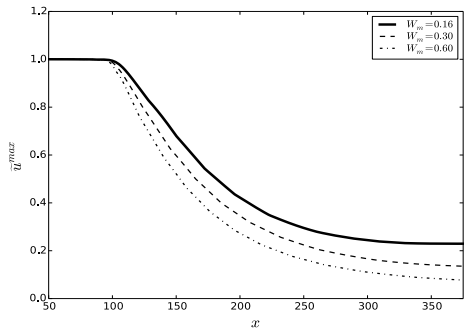

Fig. 10: $\widetilde{u}^{max}$ for different forcing amplitudes: $W_m = 0.16, 0.3, 0.6$ with $k = 0.03$

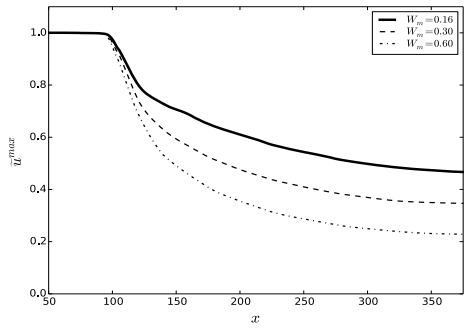

Fig. 11: $\widetilde{u}^{max}$ for different forcing amplitudes: $W_m = 0.16, 0.3, 0.6$ with $k = 0.12$

velocity (Figure 10). The trend was confirmed for different forcing wavenumber ($k = 0.12$) at multiple amplitudes (Figure 11), although the reduction is less pronounced as compared to the case with $k = 0.03$. The highest reduction in streamwise velocity fluctuations was expectedly seen for $W_m = 0.6$ and $k = 0.03$ which reduced the fluctuations to nearly 10% of the reference values.

While an optimum value for oscillation wavelength was not reached a substantial reduction in fluctuations was achieved with $k = 0.03$ with fluctuations reducing by 90% of their reference values. The turbulent kinetic energy within the volumetric box bounded by the oscillation zone was reduced by around 80% for higher amplitude cases. At an amplitude of 0.36, Ricco [27] reports total energy reduction of streamwise fluctuations of close to 80%. The energy reduction in the current study for $k = 0.03$ and $W_m = 0.36$ is about 74% suggesting that the lowest wavenumber in the study should be close to the optimum wavenumber as seen in [27].

A special case of oscillation control was found to yield some curious results at first glance. The control was implemented for the case of Blasius flow without the presence of the constant volume forcing and thereby without the presence of the low-speed streak. As seen in Figure 12, there is no change in the value of C_f between the Blasius flow case and the control case when the streak is absent and the two C_f curves overlap. In the light of this observed

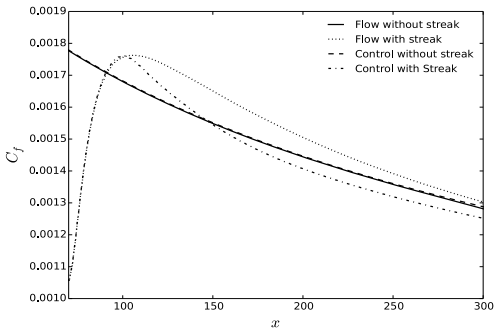

Fig. 12: Wall control ($k = 0.03$) with and without the streak.

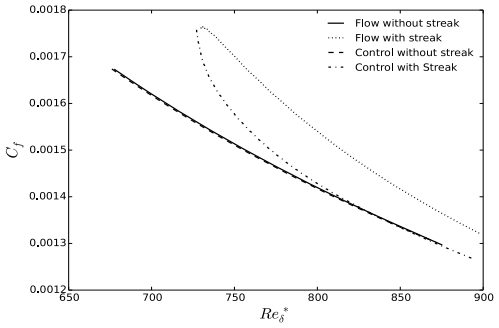

Fig. 13: Spatial development of C_f with Re_{δ^*}.

overlap, the results of Figure 5 become interesting, as the control appears to reduce the skin friction below the 2D Blasius flow value in the presence of the streak, but does not seem to do so when the streak is absent. These rather contradictory results can be reconciled when the spatial development of C_f is plotted against Re_{δ^*} as in Figure 13. The figure shows C_f values for two types of flows - laminar flow with and without the streak, and also their corresponding counterparts with spanwise flow control. The Re_{δ^*} values correspond approximately to the start and end of control region. C_f for cases without the streak expectedly overlap. The case of streak under wall control also converges to these values. On hindsight this is expected as the laminar flow with control remains largely two-dimensional. The coupling of the streamwise flow with its spanwise counterpart occurs through the fluctuating terms, which remain small for laminar cases.

5 Transition

It remains to be seen if the optimum wavenumber found for the streak continues to be effective for turbulence suppression should the flow undergo transition. In order to answer this question, time harmonic blowing and suction is used to trigger the transition to turbulence. The blowing and suction is located

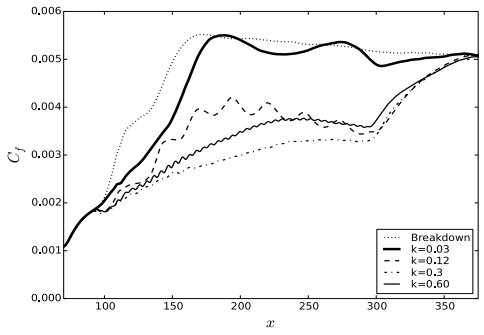

Fig. 14: C_f during transition under oscillation

within the oscillation zone to see if the oscillations are able to effectively damp out the initial growth of disturbances and if the flow is able to maintain its laminar state. The amplitude of wall oscillations was kept constant at $W_m = 0.5$ and the wavenumber was varied. In order to obtain a smoother discretization of the oscillations, the highest wavenumber studied was reduced slightly to $k = 0.6$. The wavenumber variation was thus from $k = 0.03$ to $k = 0.6$. We looked at the sharp jump in C_f which is used as a standard indicator for flow transition. Figure 14 shows the C_f values for different simulations. The dotted line indicates the case for transition without any oscillations which exhibits the sharp rise as expected.

For the case of oscillation during transition, the lowest wavenumber case ($k = 0.03$) which exhibited the maximum reduction in C_f for the laminar streak appeared to only marginally affect the wall shear stress. The friction coefficient remained oscillatory for the lowest wavenumber with its mean being close to the reference values (without oscillation). Thus, the wall oscillations with $k = 0.03$ do not suppress the viscous wall friction despite being the optimal wavenumber for diminishing the velocity fluctuations in the laminar streak flow. On the other hand, considerable reduction in the peak streamwise fluctuations was obtained as shown in Figure 15.

The parametric study of wavenumbers in the transition region reveals a trend in C_f reduction, with higher wavenumbers (at least up $k = 0.3$ as indicated in Figure 14) to causing a greater skin friction reduction. This is contrary to what was noticed during simulations of laminar streaks under oscillation where greater effectiveness appeared for lower wavenumbers. While we did not achieve an optimum wavenumber for the laminar streak cases, there appears to be a maxima reached with regards to skin friction reduction close to $k = 0.3$. Further increase in wavenumber ($k = 0.6$) reduced the effectiveness of the mechanism.

The streamwise velocity fluctuations (shown in Figure 15) were found to reduce during the transition period, although unlike the laminar streak cases, the reduction does not appear to follow a clear trend, with the reduction being oscillatory for some cases and more sustained in others.

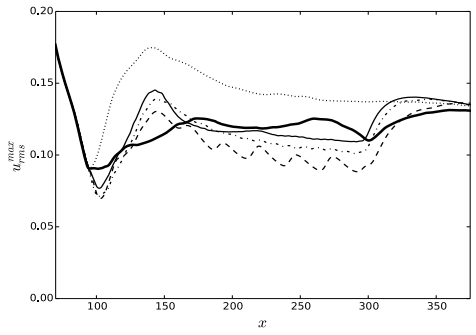

Fig. 15: Peak streamwise fluctuations during transition under oscillation. Legend as in Figure 14

The peak values for streamwise fluctuations exhibit oscillations in the streamwise direction for $k = 0.03$, 0.12 and 0.30. The oscillations are most distinctly visible for the case of $k = 0.12$. These oscillations can be explained on the basis of the streamwise variation of the spanwise velocity gradient. The maximum suppression of turbulence occurs at location with maximum spanwise gradient. Due to the spatial oscillations of the spanwise velocity, there are alternating regions of flow where the streamwise gradient of the spanwise velocity decreases to zero. In these regions the turbulence starts regenerating again in accordance with the new flow conditions. However, the sinusoidal nature of the wall forcing implies that the zero gradient region is flanked by regions of rapidly changing spanwise velocity. These regions again create the spanwise unsteadiness in the flow causing turbulence suppression. What emerges are alternating regions of turbulence suppression and regeneration. This can be verified by measuring the streamwise distance of the peaks observed in figure 16 which shows the oscillation region for transition flow under wall forcing with $k = 0.12$. For this case the streamwise distance between the consecutive peaks (marked by circles) is found to be equal to $\Delta x = 27$ which is very close to the half wavelength of the forcing ($\lambda_{forcing}/2 = 26.4$) which corresponds to the distance between two consecutive region of low streamwise gradient of spanwise velocity.

For $k = 0.30$ the oscillation amplitude is small and visible only under a magnified view (not shown). Again the streamwise separation of the peaks ($\Delta x = 10.6$) matches with the half wavelength of forcing ($\lambda_{forcing}/2 = 10.5$). This phase dependence of the streamwise fluctuations appears to reduce with higher wavenumbers. There are two reasons for this apparent reduction. Firstly, with higher wavenumbers, the streamwise distance between consecutive high gradient regions is reduced. Hence there is lesser time for turbulence to regenerate. Secondly, as the wavenumber is increased the height of the Stokes layer decreases. For all oscillation cases except $k = 0.03$, the location of the peak fluctuations is near the edge of the Stokes layer height where the amplitude of oscillations is highly diminished. The direct effect of reduced amplitude oscillations at these higher wall normal locations will be considerably small. Instead, the reduced peak values reflect the lower intensity of turbulent fluctuations

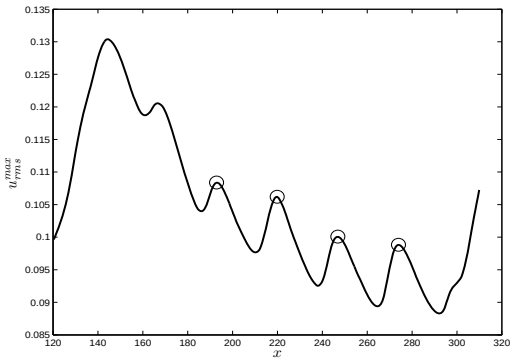

Fig. 16: Oscillatory nature of peak streamwise fluctuations for $k = 0.12$. Streamwise distance between the peaks (circles) matches the forcing wavelength

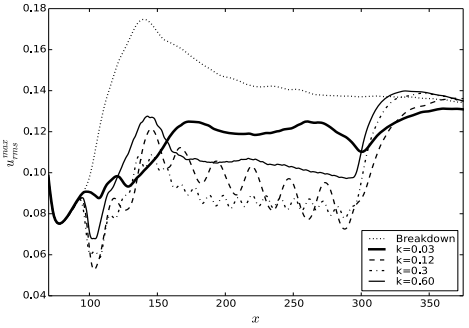

Fig. 17: Streamwise velocity fluctuations at $y = 0.5$. The phase dependence of fluctuations is more prominent at lower wall-normal locations

which are being convected away from the near wall region, where the Stokes layer has its maximum effect. This lower intensity in turn leads to a reduced turbulent production, and thus lower peak values. This can be seen by looking at the streamwise fluctuations close to the wall instead of focusing on the peak values. Figure 17 shows the u_{rms} values at $y = 0.5$ for all the cases. The phase dependence of the streamwise fluctuations is prominently evident even for $k = 0.30$. Again for an even higher wavenumber case ($k = 0.60$), the phase dependence is barely visible due to the reasons explained above, although the short wavelength oscillations can actually be observed in Figure 17.

To explore this further, the u_{rms} oscillations at different wall-normal heights are studied for their phase relationship with the spanwise velocity. Figure 18 shows the u_{rms} values at different y-locations within the control region for the case of $k = 0.3$. A Savitzky-Golay spatial filter is used to obtain the filtered signal free from the oscillations in the streamwise direction, which uses a polynomial expression to fit successive subsets of the data with a linear least square method. A polynomial of order one and with a smoothing window subset of half the wavelength of wall oscillations was found sufficient to filter out the oscillations present in the signal. The dotted lines in Figure 18 represent the smoothened signal obtained from the filter. The oscillating part of the signal, obtained from subtracting the the filtered signal from the original one,

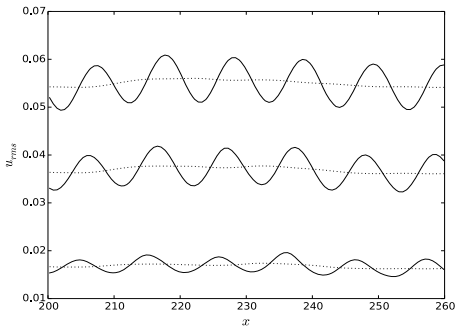

Fig. 18: Streamwise velocity fluctuations at $y = 0.1, 0.2, 0.3$ (From bottom to top) for $k = 0.3$. The filtered signal is shown with a dotted line.

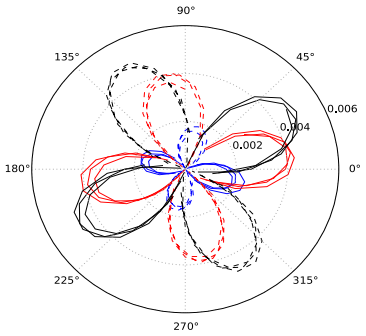

Fig. 19: Wall phase relationship of u_{rms} for $y = 0.1(blue), 0.2(red), 0.3(black)$. Solid lines represent the positive values while dashed line represents negative values.

is plotted against the wall-phase of the spanwise velocity as a polar plot in Figure 19. The positive and negative values of the fluctuating part of the signal are represented by solid and dashed lines respectively. It is evident that there is no unique relationship between the fluctuations and the wall phase of the spanwise velocity. The phase relation appears to be rotating in the counter clockwise direction as we move higher up in the wall-normal direction. However, the phase plots nearly collapse when they are plotted with the local phase of the spanwise velocity at their corresponding wall-normal locations (Figure 20).

The peak wall-normal fluctuations (v_{rms}^{max}) are shown in Figure 21 which show substantial reduction as well. Comparing the wall-normal fluctuations for the different oscillation cases with the C_f values in Figure 14, a striking qualitative correlation can be seen. The lowest wavenumber, $k = 0.03$, seems to only marginally affect both the skin friction and the peak wall-normal fluctuations with the values of both remaining close to the reference case (transition without oscillation) values. The largest reduction in both is observed for $k = 0.3$. Further increase in wavenumber ($k = 0.60$) yields rising values of both C_f and v_{rms}^{max} (although still remaining below the reference case values). Furthermore, both skin friction and peak wall-normal fluctuations for $k = 0.60$ are initially lower than the corresponding values for $k = 0.12$. However this trend is re-

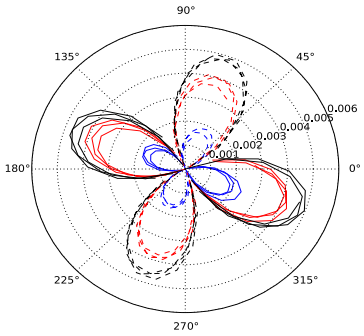

Fig. 20: Local phase relationship of u_{rms}.

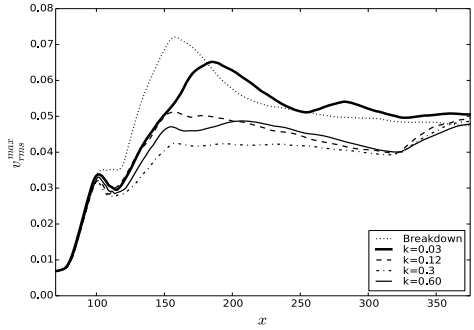

Fig. 21: Peak wall-normal fluctuations during transition under oscillation

versed further downstream with the case having $k = 0.12$ experiencing greater reductions downstream in both skin friction and peak wall-normal fluctuations. The qualitative correlation between the two quantities (C_f and v_{rms}^{max}) is striking given the lack of similar qualitative correlation between skin friction and the longitudinal velocity fluctuations.

The results of the current study can be seen in the light of a similar study by Ricco [27] using linearized theory. The prediction from the linear theory of the effect of wall oscillation is consistent with the non-linear results. This was to an extent expected. The present study extends the control region to a transitional flow case, and finds that the forcing effectiveness changes and the optimum parameters for the two flow regions are an order of magnitude apart. It becomes important to consider the results of the laminar and transition regions together, as it reminds us of the obvious drawback of the linear theory in its dependence of a fixed base state. In all scenarios where the flow undergoes a change in the base state, as in by-pass transition to name one example, linear theory ceases to be accurate and its predictions will likely fail to some degree. A recent study [15] used the linear Navier-Stokes equations for the travelling wave type wall forcing and created a phase space for the turbulent energy in the domain. The results qualitatively match the drag reduction map from DNS [25] with the same parameters. This is certainly an interesting result and

points to the dominant role played by the linear equations even in some fully turbulent flow cases. However, the linear study reported an explosive growth of solutions in regions which correspond to drag increase in the DNS study. While in this case, the growth of disturbances appears to be modelled to an extent within the linear equations, predictions made solely on the basis of linear theory would probably be highly off the mark due to the change of base state that would follow. The order of magnitude difference in the optimum parameters of the wall forcing in two different regimes presented here becomes a case in point. While the current study confirms the results of linear theory for laminar low-speed streak, the slight perturbation leads to a change in base state, and completely alters the effectiveness of the forcing in this new base state.

6 Conclusion

A parametric study of the effect of streamwise oscillations of spanwise wall velocity on a single low-speed streak has been performed showing large suppression in velocity fluctuations. The wall shear stress for the laminar streak cases was reduced slightly for all wavenumbers simulated and in two of the cases ($k = 0.03$ and $k = 0.12$) the value dropped below the laminar Blasius flow without streaks. An optimum wavelength for suppression could not be reached within the allowable oscillation parameters but the trend showed higher reduction of velocity fluctuations at lower wavenumbers. A comparison with the energy suppression values obtained by Ricco [27] suggests that the lowest wavenumber in the study ($k = 0.03$) should be very close to the optimum wavenumber. Changing the amplitude of oscillations showed a monotonic increase in velocity fluctuation reduction. The optimum wavenumber for oscillation changes, however, as the flow undergoes transition, with the new optimum wavenumber being approximately an order of magnitude larger (i.e. $k = 0.3$) than the near optimum observed for laminar streak cases. The results therefore show consistency with linear theory but departure from the linearized results once the streak is perturbed, which triggers the non-linear effects leading to transition. This eventually leads to a drastic change in the performance of the drag reducing mechanism. In the transitional region, low wavenumber cases seemed to have only a marginal affect on the skin friction for flow undergoing transition, even though the streamwise velocity fluctuations are reduced for all cases. Oscillations are observed in the peak values of streamwise fluctuations which are explained on the basis of spatially alternating regions of high turbulence suppression and turbulence regeneration in the temporary absence of a the velocity gradient. The oscillations in the streamwise velocity fluctuations at different wall normal locations have a strong phase relationship with the local phase of the spanwise velocity at the corresponding wall-normal location. A striking qualitative correlation is seen between the trends for skin friction and wall-normal fluctuations, one that merits further studies. In the present investigation, the flow was artificially disturbed to trig-

ger the transition to turbulence, hence it yet does not answer the question whether the spanwise oscillations can prevent bypass transition. However, it points towards a drastic change in efficiency of the mechanism (for the same parameters) between the laminar and transition region which would be useful to keep in mind for any practical implementation.

Acknowledgements Academic Research Fund Tier 2 (Grant No. MOE2012-T2-1-030) from the Ministry of Education, Singapore, is greatly acknowledged.

References

1. Akhavan, R., Jung, W., Mangiavacchi, N.: Turbulence control in wall-bounded flows by spanwise oscillations. Applied Scientific Research **51**(1-2), 299–303 (1993)
2. Andersson, P., Berggren, M., Henningson, D.S.: Optimal disturbances and bypass transition in boundary layers. Phys. Fluids **11**(1), 134–150 (1999)
3. Andersson, P., Brandt, L., Bottaro, A., Henningson, D.S.: On the breakdown of boundary layer streaks. Journal of Fluid Mechanics **428**, 29–60 (2001)
4. Asai, M., Minagawa, M., Nishioka, M.: The instability and breakdown of a near-wall low-speed streak. Journal of Fluid Mechanics **455**, 289–314 (2002)
5. Baron, A., Quadrio, M.: Turbulent drag reduction by spanwise wall oscillations. Appl. Sci. Res. **55**, 311–326 (1996)
6. Berlin, S.: Oblique waves in boundary layer transition. Ph.D. thesis, Royal Institute of Technology, KTH, Stockholm, Sweden (1998)
7. Brandt, L.: Numerical studies of the instability and breakdown of a boundary-layer low-speed streak. European Journal of Mechanics - B/Fluids **26**(1), 64 – 82 (2007)
8. Brandt, L., Schlatter, P., Henningson, D.S.: Transition in boundary layers subject to free-stream turbulence. Journal of Fluid Mechanics **517**, 167–198 (2004)
9. Chevalier, M., Schlatter, P., Lundbladh, A., Henningson, D.S.: Simson — a pseudo-spectral solver for incompressible boundary layer flows. Technical report, TRITA-MEK 2007:07, KTH Mechanics, Stockholm, Sweden (2007)
10. Choi, K.S.: Near-wall structure of turbulent boundary layer with spanwise-wall oscillation. Phys. Fluids **14**(7), 2530–2542 (2002)
11. Choi, K.S., Debisschop, J.R., Clayton, B.R.: Turbulent boundary-layer control by means of spanwise-wall oscillation. AIAA **36**(7), 1157–1163 (1998)
12. Dong, M., Wu, X.: On continuous spectra of the orrsommerfeld/squire equations and entrainment of free-stream vortical disturbances. Journal of Fluid Mechanics **732**, 616–659 (2013)
13. Du, Y., Karniadakis, G.: Suppressing wall turbulence by means of a transverse travelling wave. Science **288**, 1230–1234 (2000)
14. Du, Y., Symeonidis, V., Karniadakis, G.: Drag reduction in wall-bounded turbulence via a transverse travelling wave. Journal of Fluid Mechanics **457**, 1–34 (2002)
15. Duque-Daza, C.A., Baig, M.F., Lockerby, D.A., Chernyshenko, S.I., Davies, C.: Modelling turbulent skin-friction control using linearized navierstokes equations. Journal of Fluid Mechanics **702**, 403–414 (2012)
16. Hack, M.J.P., Zaki, T.A.: The continuous spectrum of time-harmonic shear layers. Phys. Fluids **24**(3), 034101 (2012)
17. Jacobs, R.G., Durbin, P.A.: Simulations of bypass transition. Journal of Fluid Mechanics **428**, 185–212 (2001)
18. Jovanovi, M.R.: Turbulence suppression in channel flows by small amplitude transverse wall oscillations. Phys. Fluids **20**(1), 014101 (2008)
19. Jung, W.J., Mangiavacchi, N., Akhavan, R.: Suppression of turbulence in wall bounded flows by highfrequency spanwise oscillations. Phys. Fluids A **4**(8), 1605–1607 (1992)
20. Laadhari, F., Skandaji, L., Morel, R.: Turbulence reduction in a boundary layer by a local spanwise oscillating surface. Phys. Fluids **6**(10), 3218–3220 (1994)

21. Luchini, P.: Reynolds-number-independent instability of the boundary layer over a flat surface: optimal perturbations. Journal of Fluid Mechanics **404**, 289–309 (2000)
22. Matsubara, M., Alfredsson, P.H.: Disturbance growth in boundary layers subjected to free-stream turbulence. Journal of Fluid Mechanics **430**, 149–168 (2001)
23. Quadrio, M., Ricco, P.: Initial response of a turbulent channel flow to spanwise oscillation of the walls. Journal of Turbulence **4**(7) (2003)
24. Quadrio, M., Ricco, P.: Critical assessment of turbulent drag reduction through spanwise wall oscillations. Journal of Fluid Mechanics **521**, 251–271 (2004)
25. Quadrio, M., Ricco, P., Viotti, C.: Streamwise-travelling waves of spanwise wall velocity for turbulent drag reduction. Journal of Fluid Mechanics **627**, 161–178 (2009)
26. Rabin, S.M.E., Caulfield, C.P., Kerswell, R.R.: Designing a more nonlinearly stable laminar flow via boundary manipulation. Journal of Fluid Mechanics **738** (2014)
27. Ricco, P.: Laminar streaks with spanwise wall forcing. Phys. Fluids **23**(6), 064103 (2011)
28. Ricco, P., Quadrio, M.: Wall-oscillation conditions for drag reduction in turbulent channel flow. International Journal of Heat and Fluid Flow **29**(4), 891 – 902 (2008)
29. Ricco, P., Wu, S.: On the effects of lateral wall oscillations on a turbulent boundary layer. Experimental Thermal and Fluid Science **29**(1), 41 – 52 (2004)
30. Schlatter, P., Brandt, L., de Lange, H.C., Henningson, D.S.: On streak breakdown in bypass transition. Phys. Fluids **20**(10), 101505 (2008)
31. Skote, M.: Turbulent boundary layer flow subject to streamwise oscillation of spanwise wall-velocity. Phys. Fluids **23**(8), 081703 (2011)
32. Skote, M.: Temporal and spatial transients in turbulent boundary layer flow over an oscillating wall. International Journal of Heat and Fluid Flow **38**, 1 – 12 (2012)
33. Skote, M.: Comparison between spatial and temporal wall oscillations in turbulent boundary layer flows. Journal of Fluid Mechanics **730**, 273–294 (2013)
34. Skote, M.: Scaling of the velocity profile in strongly drag reduced turbulent flows over an oscillating wall. International Journal of Heat and Fluid Flow **50**, 352–358 (2014)
35. Touber, E., Leschziner, M.A.: Near-wall streak modification by spanwise oscillatory wall motion and drag-reduction mechanisms. Journal of Fluid Mechanics **693**, 150–200 (2012)
36. Viotti, C., Quadrio, M., Luchini, P.: Streamwise oscillation of spanwise velocity at the wall of a channel for turbulent drag reduction. Phys. Fluids **21**(11), 115109 (2009)
37. Westin, K.J.A., Boiko, A.V., Klingmann, B.G.B., Kozlov, V.V., Alfredsson, P.H.: Experiments in a boundary layer subjected to free stream turbulence. part 1. boundary layer structure and receptivity. Journal of Fluid Mechanics **281**, 193–218 (1994)
38. Xu, C.X., Huang, W.X.: Transient response of reynolds stress transport to spanwise wall oscillation in a turbulent channel flow. Phys. Fluids **17**(1), 018101 (2005)
39. Yudhistira, I., Skote, M.: Direct numerical simulation of a turbulent boundary layer over an oscillating wall. Journal of Turbulence **12**(9) (2011)